MAX-PLANCK-INSTITUT FÜR PLASMAPHYSIK

GARCHING BEI MÜNCHEN

HEAVY IMPURITY COLLECTION AT THE PLASMA EDGE OF THE STELLARATOR W VII A

Jørgen Schou [+)]

PWW

IPP 9/38 Dezember 1981

[+)] E.C.C.-Grantee,

present address: Physics Department, Risø National Laboratory
DK-4000 Roskilde, Denmark

Die nachstehende Arbeit wurde im Rahmen des Vertrages zwischen dem Max-Planck-Institut für Plasmaphysik und der Europäischen Atomgemeinschaft über die Zusammenarbeit auf dem Gebiete der Plasmaphysik durchgeführt.

IPP 9/38 Jørgen Schou

Heavy impurity collection at the plasma edge of the stellarator W VII A

Zusammenfassung

Die schweren Verunreinigungen in der Randschicht des Stellarators Wendelstein VII A wurden mit Kohlenstoffaufsammelproben, die für bis zu zweihundert Entladungen in He exponiert waren, untersucht. Die Proben wurden anschließend mit 1 MeV $^4He^+$ Rutherford-Rückstreuung analysiert. Die durchschnittliche Belegung pro Entladung war für Mo 6×10^{10} Atome/cm^2, für Wand-Material (Fe, Cr, Ni) 1×10^{11} Atome/cm^2, und für Ti 2-4 $\times 10^{12}$ Atome/cm^2. Mit Ausnahme von Ti ist diese Belegung mit Verunreinigungen über eine Größenordnung kleiner als entsprechende Ergebnisse von vergleichbaren Tokamaks.

ABSTRACT

The presence of impurities at the plasma edge of the Wendelstein VII-A stellarator was studied by means of carbon probes that were exposed to up to 200 plasma discharges in helium. The probes were subsequently analysed with 1 MeV $^4He^+$ Rutherford Backscattering. The average impurity deposition for Ti, Mo and wall components (Fe, Cr, Ni) was $2\text{-}4 \cdot 10^{12}$ atoms/cm^2, $6 \cdot 10^{10}$ atoms/cm^2 and $1 \cdot 10^{11}$ atoms/cm^2 per discharge, respectively. With the exception of Ti this impurity deposition is more than one order of magnitude smaller than than the corresponding results from comparable tokamaks.

INTRODUCTION

The Wendelstein VII A stellarator has recently reached parameters that have been so far inaccessible for tokamaks and stellarators[1]. The stellarator has been operating in a currentless regime in which the plasma was heated by neutral injection alone. However, an accumulation of impurities in the plasma center resulted in an enhanced radiation loss, which prevented long discharges.

In the first half of 1980 mostly carbon, oxygen, and nitrogen were observed by spectroscopical methods in the deuterium-plasma. A probable origin for these light impurities are the neutral injectors. However, titanium from gettering, iron (from the first wall) and molybdenum (from the wall-protecting plates opposite to the injectors) also may be candidates. The reason for this is that more than 50% of the injection power is deposited in the plates during the initial injection phase.

In order to investigate the impurities a rotatable collector was mounted outside the plasma edge. Its purpose was to investigate whether or not impurities were present in this region and possibly to study the time dependence of the impurity flux.

Impurity collection in W VII A has been performed only for discharges in helium.

COLLECTOR

Three or six carbon stripes (papyex) were placed at a distance from the center of the plasma vessel such that the nearest

deposition area was 142 mm from the axis (Fig. 1). The stripes were mounted on a carbon cylinder, which could be rotated at 360° per second or kept in a fixed position. The stripes and the cylinder were covered by a fixed cylindrical shield of stainless steel. The particles could be deposited on the stripes through two vertical slits of 1.5 mm width in the shield. The slits were positioned perpendicular to the magnetical field, so that the ion direction and electron direction could be selected in ohmic discharges.

The stainless steel cylinder was set at wall potential, whereas the carbon cylinder was floating.

The plasma cross section in W VII A is elliptical with the major axis rotated 45° from the horizontal plane at this position. The ratio of the major (2a) and minor axis (2b) is determined by the external transformation ι_0 and the effective plasma radius $\bar{a}$ via

$$\frac{a}{b} = ((1 + \sqrt{(4/5)\iota_0})/(1 - \sqrt{(4/5)\iota_0}))^{1/2}$$

and

$$\bar{a} = (ab)^{1/2} .$$

The closest distance from a papyex stripe to the plasma edge has been evaluated numerically in the cases considered.

Before a day of experiment a Ti-ball was placed in the center of the torus at the same azimuthal position as the collector (#6), and gettering performed with approximately 50-mg Ti for a period of about ten minutes.

METHODS OF ANALYSIS

The papyex stripes were analysed at the 2.5 MeV accelerator after exposure to a number of discharges in W VII A.

An attempt was made to utilize ion-induced X-rays due to primary H^+ or He^+-ions. This method turned out to be insufficient because of too large background peaks from the carbon itself which were close to expected values for impurities.

Rutherford Backscattering Spectrometry[2] was then used with 1 MeV $^4He^+$ and 1.5 MeV $^{14}N^+$ (Fig. 2). Because of the larger cross section for backscattering with nitrogen ions RBS with nitrogen was a factor of 3.6 more sensitive (for Pt) than with helium ions. On the other hand, the half-width for nitrogen ions was a factor of 2.4 larger than that for helium ions. Combined with the much smaller nitrogen currents (10-15 nA), this meant that an analysis with 1 MeV $^4He^+$ was most advantageous. In this case the beam current was 5 times larger.

The backscattered helium ions were energy-analysed by a semiconductor detector set at an angle of 165° with respect to the beam direction. The sensitive area of the detector corresponded to a solid angle of $1.74 \cdot 10^{-4}$ sr, and a characteristic beam current was 50 nA. For the first series (W7/3/1) of measurements the ion doses were about 200 μC. At all later series the analysing doses were increased to approximately 1 mC.

A clear disadvantage of RBS is the poor mass resolution for heavy impurity atoms. For example, it was impossible to distinguish among Ta-, W- and Au-atoms, and among the stainless steel components Fe-, Cr-, and Ni-atoms. On the other hand, once a specific peak in a backscattering spectrum has been determined, the absolute surface impurity density is immediately obtained.

Papyex was used as collector material because of its flexibility and also because the impurity content of heavy atoms was low. Deposited atoms no lighter than Ti-atoms could be distinguished from the impurity background of the papyex.

For the atoms considered here there was a relatively uniform, "peakless" background corresponding to area densities listed in Table 1. One notes that these "area densities" were of the same order of magnitude or larger than the impurity densities deposited on the stripes in the discharges.

A spectrum from the test series (W7/6/1^+) is shown in Fig. 3. The corresponding spectrum from the same papyex stripe without exposition to the plasma has been indicated below some of the peaks. One notes the clear Ti-, Mo-, O- and N-peaks, but the surface density of the stainless steel components may also be determined within a satisfactory accuracy. The uniform background below channel 125 has not been been identified. For the moment it is not clear whether these light impurities (S and/or Cl) have been present in the papyex, almost homogeneosly distributed in depth, or whether the impurities are deposited during the discharges.

In connection with the large He^+-ion doses sputtering from papyex may occur. 1 mC corresponds to $8 \cdot 10^{17}$ He-atoms/cm^2, which would lead to sputtering of 1-2 monolayers with an estimated sputtering coefficient of 0.005 for 1 MeV He on carbon. However, it is quite clear from Table 2 that the detected impurity counts per charge unit do not decrease with increasing dose. This means that no sputtering of impurities had taken place during the analysis.

RESULTS

The origin of the possible impurities has been listed in Table 3. In all the analysed cases only the stripe closest to the plasma was investigated. The distance to the torus center was always 142 mm. It is expected that the impurity

flux increases with decreasing distance to the plasma edge[3-5].

Only the ion side was investigated. A tentative analysis of the electron side revealed no observable impurity deposition.

The series W7/3/1 (first stripe of third collection) was time-resolved during the discharges. The stripes were exposed to about 200 discharges, which corresponds to an equivalent surface density from 10 discharges without rotating the collector. Only an upper limit could be found here.

In the series with fixed collector the sensitivity was raised by a factor of 20. This way of increasing the impurity deposition turned out to be quite successful. The result and the corresponding plasma parameters are listed in Table 4. In the series W7/4/1$^+$ - W7/6/1$^+$ the impurity density has been determined by subtracting the number of counts at a non-exposed area on the same stripe from the number of counts at the exposed area.

The impurity collection was performed at the series W7/4/1$^+$ and W7/5/1$^+$ through an aperture in the protection shield (width 1.5 mm, shield thickness 1.0 mm). In the latter series the stainless steel shield was covered with a gold layer of 1-µm thickness.

Wherever the impurity densities are listed in the results (Table 4) the upper row is the total surface density, whereas the lower row is the average density per discharge.

The Mo-density in the series W7/4/1$^+$ and W7/5/1$^+$ is surprisingly similar, although the plasma currents, the external transformations ι_0 and the ion temperatures are somewhat different. This could mean that $6 \cdot 10^9$ Mo-atom/(cm^2·discharge) is a characteristic impurity deposition corresponding to these kinds of geometry and discharges.

In W7/5/1^+ the influence of the shield material was studied. The gold-coverage of the shield in this series reduced the deposition of Fe, Cr, and Ni by a factor of 7. It is a clear indication that stainless steel has been sputtered from the the edge of the aperture onto the carbon stripe. Such aperture sputtering in plasma experiments has been reported recently[6].

On the other hand, a uniform Au-background in W7/5/1^+ was observed. The atomic density was approximately 10^{-5} times the carbon density, and the depth of the Au-distribution was more than 0.5 μm. The diffusion of gold from a papyex surface into the bulk has turned out to be negligible, even at elevated temperatures. A possible explanation is material transfer in submicron grains from the aperture to the bulk of the papyex via arcing or a similar mechanism[7].

In the last series, W7/6/1^+, the shield with the 1.5-mm slit was replaced by a stainless steel shield with an opening of 16 mm corresponding to a solid angle of 2π. For a single-charged molybdenum ion of kinetic energy 10 eV the gyroradius is approximately 0.5 mm, which is comparable to the width of the slit. It is, therefore, expected that the impurity deposition would be enhanced without aperture[8].

The electron density in this series was somewhat reduced, whereas the ion temperature was increased. This latter change may lead to an enhanced impurity flux, but the increase by a factor of 10 in the Mo-atom deposition cannot be explained by the larger ion temperature in W7/6/1^+ alone. Also the Fe, Cr, and Ni deposition is increased by a factor of 10 compared with W7/5/1^+. This enhancement suggests that a majority of the gyrating particles does not pass the aperture, so that a considerable fraction of the heavy ions are in low charge states at the plasma edge.

The area densities for Cu and Zn are relatively uncertain because of poor peak determination, and should be considered more as an upper limit. This is also the case for the heaviest impurities Au and Ta.

The Ti-peak is determined relatively well. In all the series considered the titanium originates clearly from the papyex exposition to the plasma, and not from diffusion in connection with gettering. This follows from the total absence of any Ti more than a few mm away from the slit in the time-resolved measurements that were performed with the same aperture geometry as in W7/4/1$^+$ and W7/5/1$^+$. However, the density on W7/4/1$^+$ is somewhat uncertain and should be regarded more as an upper limit. In the series W7/6/1$^+$ an increase by more than a factor of 20 relative to W7/5/1$^+$ is observed. At the same time, it is surprising that the Ti-density in W7/6/1$^+$ varies with a factor of 2 over a lateral distance of 4 mm. In fact, later measurements indicate that such a lateral variation of the Ti-density occurs rather frequently[9].

Also the oxygen density (with subtracted carbon background) has been indicated in the Table. It is unclear whether this density enhancement relative to the unexposed papyex area originates from the plasma, from oxydation of low-Z materials on the stripe during the exposure to air or water deposition on the stripes during the exposure to air.

COMPARISON TO TOKAMAKS

The deposition rate abundance of heavy impurities in W VII A is compared to tokamaks, at which similar measurements were performed without an aperture[4,8,10] (Table 5). One notes that the collected Mo-, Fe-, Cr-, and Ni-density are

are much smaller in W W VII A than in PULSATOR, which even had considerably lower ion temperature and no neutral injection. Obviously, the smaller distance to the plasma in PULSATOR and the changed collector geometry may play a role, but for both kinds of impurities the density is more than a factor of 20 lower in W VII A. This may hardly be explained alone by the difference in distance and geometry.

Compared to DITE and TFR 600 the heavy impurity density in W VII A is surprisingly small as well.

CONCLUSION

In the presentation of data it has been assumed that the collected impurity density is proportional to the number of discharges. Erosion and saturation effects have been reported for TFR[3] and DITE[11]. It would, therefore, be desirable to make a few impurity collections under similar plasma parameters in order to study the density dependence on the number of discharges. Since no collector erosion was found on PULSATOR[3], the impurity deposits for W VII A have merely been divided by the number of discharges. However, it is, of course, substantial for any comparison that the impurity per discharge is available.

Unfortunately, it was impossible to study the radial dependence, for practical reasons. Since it is well known from measurements in the scrape-off layer of tokamaks that the impurity density collected depends strongly on the distance to the plasma[3,4,5], it would be essential to know this dependence. In addition, it would be important to study the influence of the external transformation, as the precise dis-

tance to the plasma is determined by the ratio of the helical current to plasma current.

In particular, time-resolved measurements during the non-current-free operation of W VII A would be desirable. So far, no significant concentration of heavy impurities could be observed in the center by spectroscopic methods. This may indicate either efficient screening for the impurities or slow transport at these conditions.

For a comprehensive understanding of the impurity fluxes at the plasma edge it seems necessary to perform additional measurements with a collector in other positions. The present position (#6) has the advantage that it is in a neutral injection plane. On the other hand, it is uncertain how the Mo-deposit is influenced by the limiter position.

Generally, it would be desirable to gather a larger amount of impurity data than presented here. The dependence on the plasma parameters has hardly been touched upon in the present work. Also the question of whether or not light impurities, e.g. Cl or S, are present at the plasma edge has not been answered.

In summary, the first study of heavy impurity collection at the plasma edge in a stellarator has been performed. The amount of collected impurities in W VII A was smaller than in comparable tokamaks.

ACKNOWLEDGEMENTS

This work has been supported by a grant from the Commission of the European Communities. The hospitality at IPP-Garching is acknowledged. The author thanks R. Behrisch for suggesting the project, and appreciates the support from and the discussions with H. Renner and B.M.U. Scherzer. He also thanks J. Bömerl from W VII A and the technical staff at the 2.5-MeV accelerator for valuable assistance.

TABLE 1
PEAKLESS BACKGROUND
IN CLEAN PAPYEX
(1 MeV $^4He^+$, 1.2 mC)

"Background impurity"	Counts	Corresponding surface density
Ta, W, Au (M_2 > 170 amu)	40	< $9 \cdot 10^{11}$ atoms/cm^2
Mo	16	< $1.3 \cdot 10^{12}$ atoms/cm^2
Cu, Zn	10	< $1.7 \cdot 10^{12}$ atoms/cm^2
Fe, Cr, Ni	86	< $1.2 \cdot 10^{13}$ atoms/cm^2
Ti	170	< $3.0 \cdot 10^{13}$ atoms/cm^2

TABLE 2

IMPURITY DETECTION AS A FUNCTION OF DOSE

(1 MeV $^4He^+$)

Impurity	Dose (μC)	Counts	Counts per unit dose (counts/μC)
Mo	264	12	0.045
	530	34	0.064
	869	59	0.068
Fe, Cr, Ni	264	22.5	0.085
	530	34	0.064
	869	75	0.086
Ti	264	232	0.879
	530	449	0.847
	869	791	0.910

TABLE 3
ORIGIN OF IMPURITIES

Ti	Gettering before experiments performed at the same azimuthal position; gettering in neutral injectors.
Fe, Cr, Ni	First wall
Cu	Aperture of neutral injectors
Mo	Limiter, 135° away from the collector; Armour plates opposite to the injectors
Ta	Filaments in neutral injectors
Au	Coverage of a few antennas.

Comment: Injector C operates at the same azimuthal position (#6) as the collector.

TABLE 4
IMPURITY COLLECTION

Series[a)]	W7/3/1 200 disch. time-resolved	W7/4/1+ stainless steel apert.	W7/5/1+ gold-covered apert.	W7/6/1+ no aperture
Date		18.2.81 20.2.81	27.2.81 2.3.82 11.3.81	19.3.81
Number of disch.	Eq. 10	175	221	77
nõ		24902-72 24973-25073	25176-255 25273-341 25366-437	25458-534
Gas	He	He	He	He
Plasma current I_p (kA)	8-40	35	20	20
Toroidal field B_T (T)	3.5	3.5	3.5	3.5
Eff. plasma radius ā (cm)		10.4	10.0	9.5
External transf. ι_o	0.14	0.14	0.23	0.29
Closest distance to plasma (cm)		4.3	4.9	5.3
Central temp. (eV)				
Electr. $T_{e,o}$	190-470	350	450	500
Ions $T_{i,o}$	120-250	400	500	650
Central electr. density $n_{e,o}$ (10^{13} cm^{-3})	1-5	8	8	6

Continued

Continued

	W7/3/1	W7/4/1+	W7/5/1+	W7/6/1+	
Neutral injectors	none	B + C	A + B + C	A + C[b)]	
Impurity densities (atoms/cm^2)					
Heavy (Au,Ta etc) total	$<2.8\cdot10^{12}$	$3.2\cdot10^{11}$	Au-back-ground	$5.1\cdot10^{11}$	$5.4\cdot10^{10}$
per disch.	$<2.8\cdot10^{11}$	$2.1\cdot10^{9}$	$N_{Au} \approx 10^{-5}N_C$	$6.7\cdot10^{9}$	$7.1\cdot10^{8}$
Molybd. total	$<1.5\cdot10^{13}$	$1.0\cdot10^{12}$	$1.3\cdot10^{12}$	$4.6\cdot10^{12}$	$4.5\cdot10^{12}$
per disch.	$<1.5\cdot10^{12}$	$5.7\cdot10^{9}$	$6.0\cdot10^{9}$	$6.0\cdot10^{10}$	$5.9\cdot10^{10}$
Wall comp. (Fe,Cr,Ni) total	$<1.0\cdot10^{14}$	$1.4\cdot10^{13}$	$3.0\cdot10^{12}$	$1.0\cdot10^{13}$	$7.6\cdot10^{12}$
per disch.	$<1.0\cdot10^{13}$	$8.0\cdot10^{10}$	$1.4\cdot10^{10}$	$1.3\cdot10^{11}$	$1.0\cdot10^{11}$
Cu,Zn total	$<1.0\cdot10^{13}$	$8.3\cdot10^{12}$	not	$1.3\cdot10^{12}$	not
per disch.	$<1.0\cdot10^{12}$	$4.7\cdot10^{10}$	observed	$1.7\cdot10^{10}$	observed
Titanium total	-	$4.8\cdot10^{12}$	$2.0\cdot10^{13}$	$1.4\cdot10^{14}$	$2.8\cdot10^{14}$
per disch.	-	$2.7\cdot10^{10}$	$9.3\cdot10^{10}$	$1.9\cdot10^{12}$	$3.7\cdot10^{12}$
"Oxygen"	-	$5.7\cdot10^{14}$	$1.4\cdot10^{14}$	$1.4\cdot10^{15}$	$1.4\cdot10^{15}$
(background subtr.)	-	$3.3\cdot10^{12}$	$6.5\cdot10^{11}$	$1.9\cdot10^{13}$	$1.8\cdot10^{13}$

a) + means only three stripes, but the distance to torus center is constant in all cases.
b) two spots with distance 4 mm.

TABLE 5
COMPARISONS WITH TOKAMAKS

Device	Pulsator	DITE[a]	TFR 600	W VII A
Reference	9	4	3	(W7/6/1+)
Major rad. R (cm)	70	112	98	200
Gas	H_2	H_2	H_2	He
Plasma current I_p (kA)	40	50	200	20
Toroidal field B_T (T)	3	0.9	4	3.5
Central temp. (eV)				
Elec., $T_{e,o}$	800	230	1000	500
Ions, $T_{i,o}$	340	?	650	650
Central elec. density 10^{13} cm^{-3}	15	0.9	10	6
Pulse length t (ms)	120	<300	180	200
Limiter dist. a (cm)	11	26	20	13.5[b]
Lim. material	Mo	Mo	Inconel	Mo
Collector distance to plasma r-a (cm)	2	4	3	5.3[c]
Aperture	no	no	no	no
Collection direction	$\parallel B_T$	$\perp B_T$	$<45^o$ against B_T	$\perp B_T$
Neutral injection	no	no?	no?	100 kW
Mo-atoms cm^2·disch	$1 \cdot 10^{12}$	$1 \cdot 10^{14}$	-	$6 \cdot 10^{10}$
Fe,Cr,Ni-atoms cm^2·disch	$4 \cdot 10^{12}$	$1 \cdot 10^{14}$	d)	$1 \cdot 10^{11}$
Cr,Ni-atoms cm^2·disch			$1 \cdot 10^{15}$	

a) without diverter operation
b) effective plasma radius: 9.5 cm
c) minimum distance to separatrix
d) first-wall material is inconel

REFERENCES

1) D.V. Bartlett et al., in: "Plasma Physics and Controlled Nuclear Fusion Research", IAEA, Vienna, 1981, p. 185.

2) W.-K. Chu, J.W. Mayer and M.-A. Nicolet, "Backscattering Spectrometry", Academic Press (1978).

3) G. Staudenmaier, P. Staib, G. Venus and TFR-Group, J. Nucl. Mat. 76-77, 445 (1978).

4) G. Dearnaley, G.M. McCracken, J.F. Turner and J. Vince, Nucl. Instr. Meth. 149, 253 (1978).

5) G. Staudenmaier, P. Staib and S.M. Rossnagel, Bull. Am. Phys. Soc. 25, 876 (1980).

6) S.K. Erents, E.S. Hotston, G.M. McCracken, C.J. Sofield and J. Shea, J. Nucl. Mat. 93-94, 115 (1980).

7) The experiment has been performed by B.M.U. Scherzer. Also the grain transfer mechanism was suggested by B.M.U. Scherzer.

8) G. Staudenmaier, P. Staib and W. Poschenrieder, J. Nucl. Mat. 93-94, 121 (1980).

9) The analysis (with an annular detector) has been made by B.M.U. Scherzer.

10) P. Staib and G. Staudenmaier, J. Nucl. Mat. 63, 37 (1976).

11) E.W. Thomas, J. Partridge and J. Vince, J. Nucl. Mat. 89, 182 (1980).

FIGURE CAPTIONS

Fig. 1. Cross section of the collector plane.

Fig. 2. Schematic survey of Rutherford Backscattering at the 2.5 MeV accelerator.

Fig. 3. Spectrum of W7/6/1^{+} (right column in Table 4).

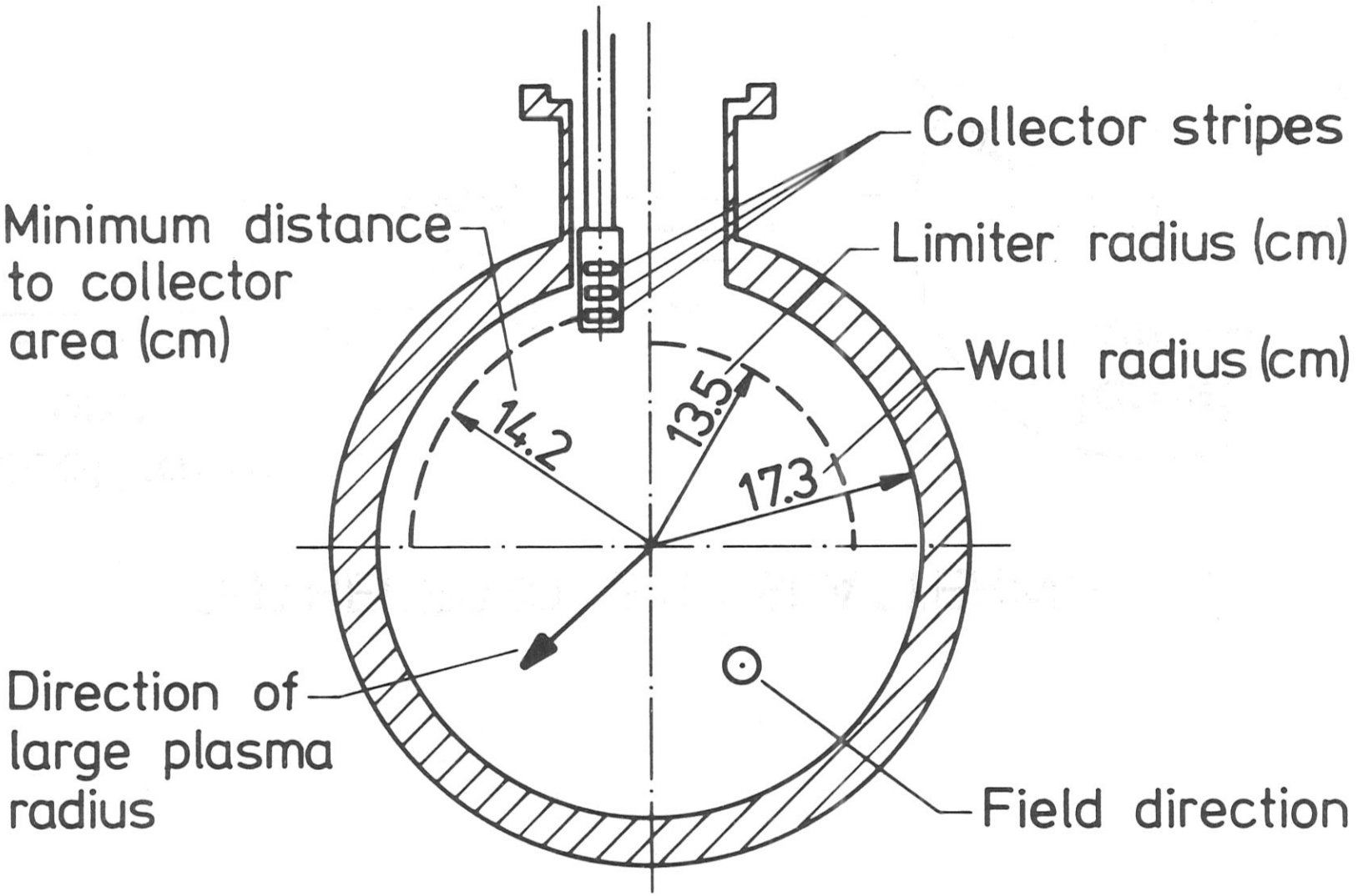
COLLECTOR GEOMETRY AT WVII A
Collector stripes
Minimum distance to collector area (cm)
Limiter radius (cm)
Wall radius (cm)
14.2
13.5
17.3
Direction of large plasma radius
Field direction

Fig. 1.

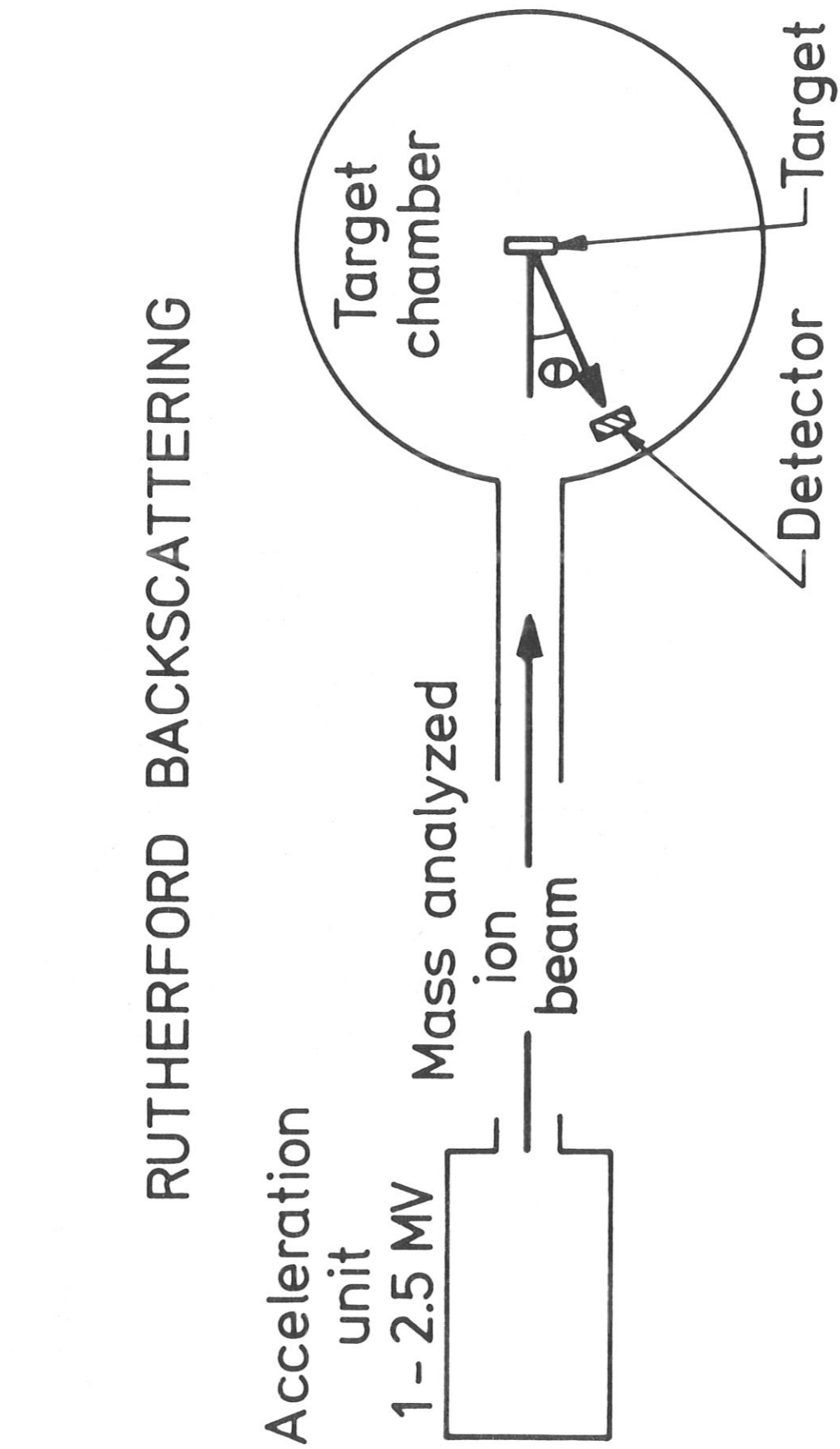
RUTHERFORD BACKSCATTERING
Acceleration unit 1-2.5 MV
Mass analyzed ion beam
Target chamber
Target
Detector
θ

Fig. 2.

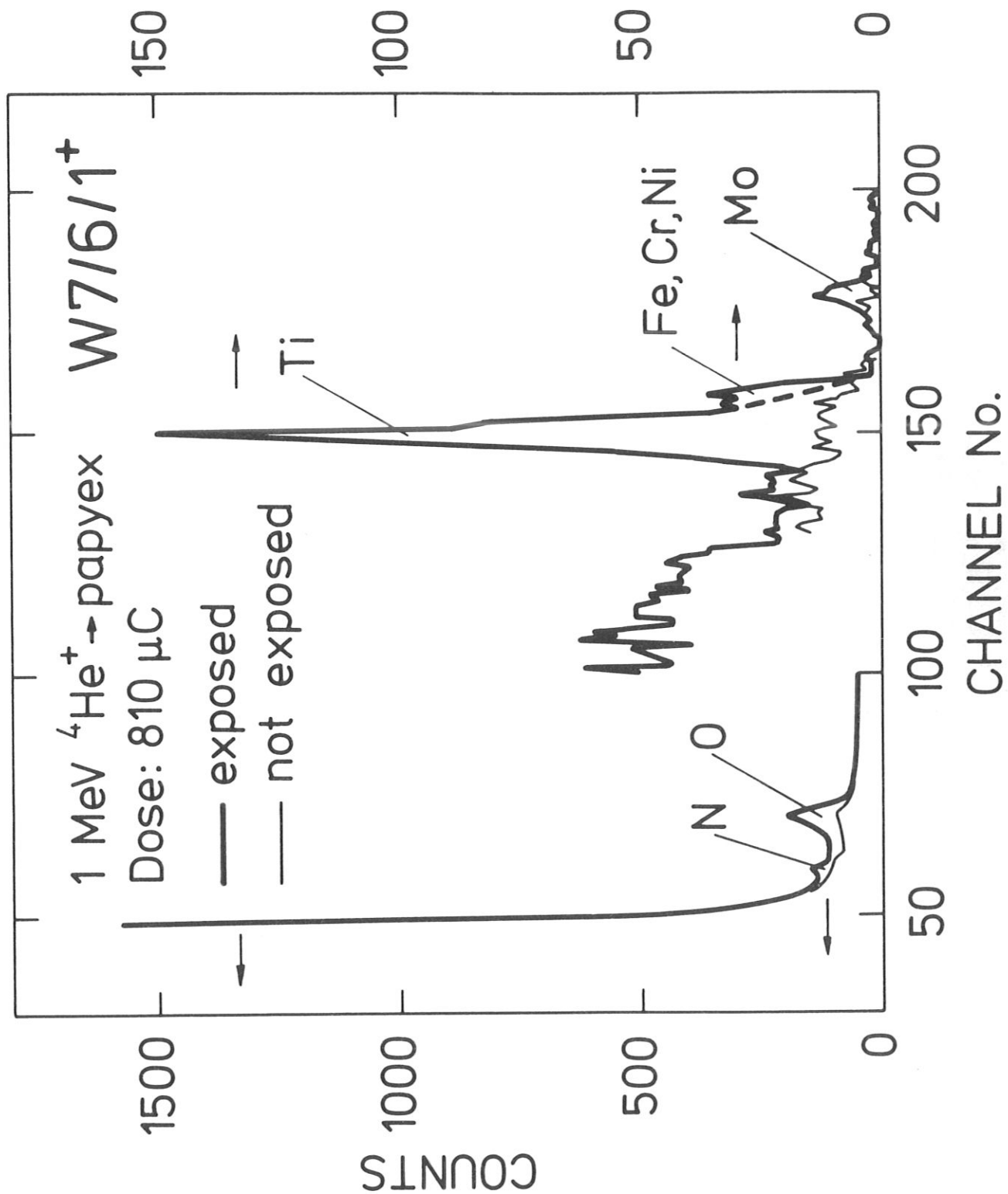
W7/6/1+
1 MeV 4He+→papyex
Dose: 810 µC
exposed
not exposed
Ti
Fe, Cr, Ni
Mo
O
N
COUNTS
CHANNEL No.
1500
1000
500
0
150
100
50
0
200

Fig. 3.